Автономная некоммерческая организация высшего образования
«Университет Иннополис»
(АНО ВО «Университет Иннополис»)

ВЫПУСКНАЯ КВАЛИФИКАЦИОННАЯ РАБОТА
(МАГИСТЕРСКАЯ ДИССЕРТАЦИЯ)
по направлению подготовки
09.04.01 – «Информатика и вычислительная техника»

GRADUATION THESIS
(MASTER GRADUATE THESIS)
Field of Study
09.04.01 – «Computer Science»

Направленность (профиль) образовательной программы
«Робототехника и компьютерное зрение»
Area of specialization / academic program title:
«Robotics and computer vision»

Тема / Topic

Разработка шестиосевого датчика силы на основе оптического датчика давления барьерного типа

Development of a six-axis force sensor based on a barrier-type optical pressure cell

Работу выполнил /

Thesis is executed by

Степанова Анастасия Антоновна

Stepanova Anastasiia Antonovna

подпись / signature

Руководитель выпускной квалификационной работы /

Graduation Thesis Supervisor

подпись / signature

Консультанты / Consultants		подпись / signature

Иннополис, Innopolis, 2024

Contents

Abstract

The multi-axis force sensor market is currently dominated by strain gauge sensors, but other options exist, such as hall-effect, fiber Bragg grating (FBG), and optoelectronic cells.

The optoelectronic cell is perceptible due to its low cost, excellent precision, and simple implementation. Nevertheless, a dearth of solutions appropriate for large-scale manufacturing and enable adjustable sensor parameters exists.

This study aims to explore how the shape and material of the barrier affect the measurement range of an optoelectronic barrier-type sensor. Additionally, a modular multi-axis force sensor will be designed using the measurement cells.

The study design involves examining the impact of barrier shape and material on the measurement range of the optoelectronic barrier-type sensor. Additionally, in the research, I designed a modular multi-axis force sensor based on the presented measurement cells.

The optoelectronic six-axial force sensor, which is the focus of this study, is characterized by its simplicity and ease of implementation as a modular sensor. It provides a cost-effective solution and facilitates the straightforward replacement of construction elements. Consequently, this sensor has the potential to broaden the range of applications for multi-axis force sensors.

This research contributes to understanding how the shape and material of the barrier affect the measurement range of optoelectronic barrier-type sensors. The design of a modular multi-axis force sensor provides a cost-effective and adjustable solution for various robotic applications.

Chapter 1

Introduction

Multi-axial force sensors, also referred to as multi-axis force sensors, are devices that can measure forces and torques in multiple directions or axes simultaneously (from one to six dimensions). These sensors find applications in various fields such as robotics, biomechanics, and industrial automation [1].

The classical multi-axis force sensor is a system of uniaxial pressure sensors of different dimensions. While the strain-gauge sensor remains the most common solution as uniaxial pressure measurement cell in the field of multi-axial force sensors, optical sensors shows noticeable accuracy with higher linearity [2]. The structures of the optical multi-force sensors has been solid [2], [3], while for strain-gauge based sensors fully mechanically decoupled solutions exists [4], [5].

The objective of this project is to investigate the relationship between the linearity of optical sensors and the construction of the barrier and multi-axial sensor configuration. The project is divided in two parts: development of a single degree of freedom pressure sensor and a multi-axis force sensor based on a designed pressure cell. Both parts aim to develop a mathematical model for the sensor, its prototype and conduct testing to evaluate accuracy, hysteresis and axis crosstalk.

The multiaxis force sensor development is ...

The most common solutions for multi-axial force sensors constructions and pressure cells types are described in the

1.1 Overview of thesis contents

Literature Review chapter will outline the general information about multi-axial force sensors, force measurement cells technologies and state pros and cons of multi-axial force sensors existing solutions. Also the chapter will review methods of statical calibration and experimental setups used for testing the sensor' kind.

Optical modeling chapter will provide the mathematical model of the optical force measuring cell.

Construction modeling will present the target multi-axis sensor structure.

In Implementation chapter I describe the experimental setup and the results evaluation techniques, provide comparison with my mathematical model.

Chapter 2

Glossary

cell of a sensor	...
coupling	...
crosstalk	undesired measured output of a transverse channel under defined load on the calibrated axis ISO 21612:2021(E)
cross-coupling	...
ERSG	Electrical Resistance Strain Gauge
FBG	Fiber Bragg grating
Data acquisition (DAQ)	the process of measuring an electrical or physical phenomenon, such as voltage, current, temperature, pressure, or sound. standards.

Chapter 3

Literature Review

3.1 Navigation

The objective of this chapter is to conduct a literature review on the development of six degrees of freedom (DOF) force sensors. In Section 3.4, an examination of the construction of multi-axial load sensor beams is presented. Section 3.5 defines the types of pressure sensors used as measurement cells for multi-axis force and torque sensors, along with their limitations.

Finally, in Section 3.6, the research gap in this field is identified.

3.2 Metrics

stiffness, nominal values, isotropy In a coupled sensor an axis force component produces signal in more then one measurement cell, therefore calibration becomes more complicated.

3.2.1 Coupling

One of the main metrics for multi-axial force sensor is degree of coupling, which determines the complexity of calibration matrix of a sensor [1], [4], [6]. Dimensions coupling problem is one of the most common problems for multi-axial force sensors [7]. The degree of coupling among the axes directly impacts the accuracy of the sensor and the complexity of calibration [1], [4], [6]. In a coupled sensor, an axis force component can produce signals in more than one measurement cell, thereby complicating the calibration process. However, designing and manufacturing highly decoupled structures can be challenging [8].

To reduce axis dependence one may change structure of the sensor or perform high precision calibration. Existing solutions for multi-axial force sensor structures are presented in the 3.4 section.

3.3 Calibration

The multi-axis calibration has static and dynamic methods based on the applied force/pressure [9], [10]. A load usually is said to be static, if it remains constant during the measurement process. Accordingly, a load is said to be dynamic if it varies significantly in a short amount of time, usually, several times during the measurement. The dynamic calibration is applied to sensors designed for highly dynamic environment with pressure pulsations or to determine the sensor response time [10]. In my research the static calibration is sufficient, therefore, lets focus on the methods used in the multi-axis force sensors development.

Two static calibration methods exists: traditional and neural-networks based [7], [11].

Traditional method involves linear transformation (LT) of pressure cells output to the force and torque space using least-square-method (LSM) [11]. The mapping is represented with $N \times 6$ matrix, where N - number of uniaxial pressure sensors of the system [11]. The method defines two limitations [11]:

- The LT defines the linear dependency of sensor' output to the elastic body transformation.
- Matrix mapping representation requires load axes independence.

In other words, the sensor output has to be linear to applied load with fully decoupled axes. The conditions are hard to satisfy, therefore many researches about structural sensors decoupling exists [4], [5], [8], [12].

Neural-networks based

…

3.3.1 How the ISO standart determines the calibration process

— All force and moment channels are measured during the calibration process of each axis. All channels are to be offset corrected in unloaded condition prior to the calibration test.

For force loading the force is applied within the neutral axes of the load cell.

In order to keep accuracy and to prevent misalignment it should be avoided to exert torque within the mounting plane between load cell and fixture. This load case should be last in the sequence. It can cause rotation of the load cell within the fixture. Thus subsequently exerted loads can be shifted from the intended load axis

misalignment determination

For a loading in discrete steps or a continuous loading procedure, the output voltages in [mV/V] of all transverse channels need to be recorded. After the calibration of all axes, the current sensitivities of these channels are known and can be used for the calculation of the crosstalk as percentage of the transducer axis' calibration range. For the force and moment channels, the transverse channels' output voltage recorded in [mV/V] (see NOTE 1) shall be converted to the physical dimension force or moment by applying the current sensitivity determined from the calibration test before.

3.4 Constructions

Typically, the assessment of forces and moments in various directions is achieved by utilizing multiple strain-sensitive sensors affixed to a flexible substrate [1]. The structure of a sensor plays a crucial role in its design as it governs characteristics such as stiffness, nominal values, isotropy, and the coupling among the measured axes [1], [12].

To create optimized decoupled structures, engineers employ finite element analysis (FEM) [1], [3], [12].

1. Rigid jointed cross-beams

The most prevalent type of sensors used are rigid-joined sensors, primarily due to their solid beam structure, which facilitates simplified manufacturing. According to studies conducted by [1], [12], rigid-joined cross beams exhibit reduced measurement isotropy and an increased level of coupling. The high level of coupling of rigid-joined sensors pushed researchers to find mechanically decoupled solutions.

A comprehensive compilation of rigid-joined cross-beam sensors can be found in [1].

2. Flexible jointed cross-beams

The flexible jointed structure was created to avoid the calibration complexity of mechanically coupled sensors [8]. Want is a flexible joint of the cross-beam? Some researches define the flexible joint as a thin regions in the beam structure. Those regions are elastic compared to the whole beam, therefore they act as a damper and reduce the cross dimension coupling.

The second type of flexible jointed cross-beams is the $WHICH_WORD_TO_USE$. Their constructions has additional mechanical component as joint, for example, bearings or hinges.

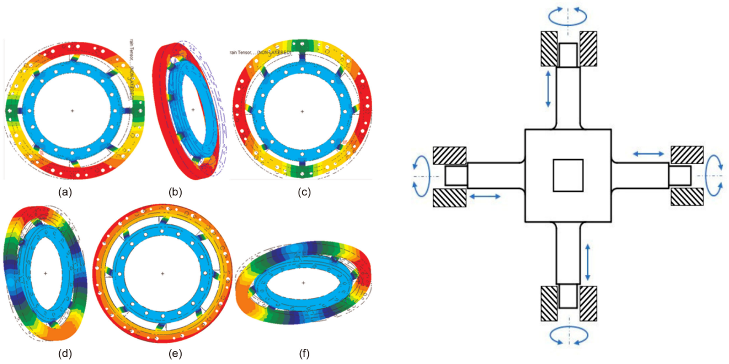

thin joints sliding joints

Figure 3.1: Example of flexible joined beams structures for multi-axial sensors.

3. Modal cross-beams

With the advancement in computational power, the creation of mechanically decoupled solutions has become more accessible. In their study, Mayetin and Kucuk [5] developed a modal sensor with an average interference error of less than 3%. This approach allows for the replacement of failed structural elements, enhancing the overall reliability and longevity of the sensor.

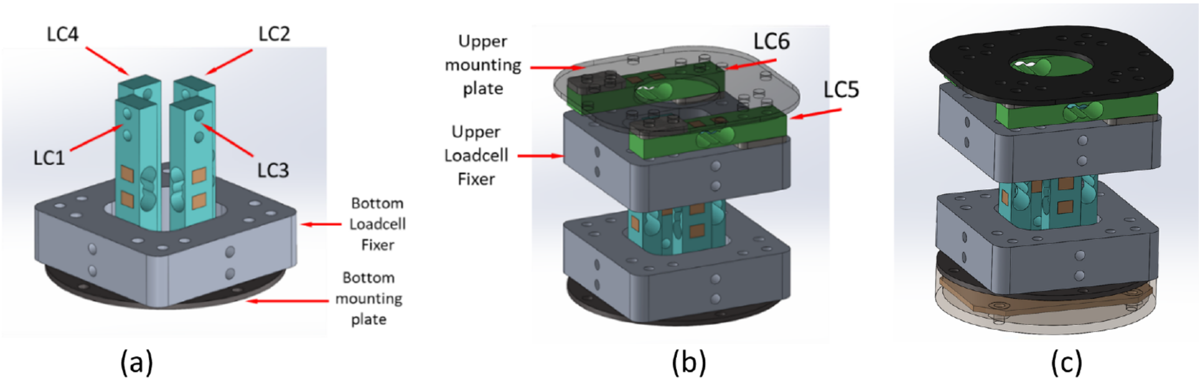

Fig. 3. Design details of the force-sensing unit, a) beam type load cells for *X* and *Y* axes, b) beam type load cell for *Z* axis, c) full assembly appearance

modal sensor from [5]

3.5 Pressure cells types

3.5.1 Electrical Resistance Strain Gauge

The principle behind Electrical Resistance Strain Gauges (ERSGs) is the change in resistance caused by deformation, as explained in a study by official representative of Keller AG manufacturer [13]. Stretching or compressing of the piezoresistive material results in a change in the electric resistance of the sensor [1]. In order to accurately measure small changes in geometry, strain-gauge sensors are typically connected to a Wheatstone bridge.

Since the creation of the multi-axis force sensor in the 1970s, the strain-resistive pressure sensor has remained a classic measuring device [14]. However, these solutions tend to be expensive and require additional surface treatment of the substrate, as well as high-quality technology for bonding with a strain-resistant component [15], [16]. Load cells, which utilize strain gauges, face challenges in signal processing. These challenges include sensitivity to temperature and magnetic noise, the need for regular calibration, and difficulties in maintenance after the substrate undergoes plastic deformation. Regarding response times, typical values of this measuring principle range from 1 to 10 ms. [10]

3.5.2 Fiber Bragg grating

Fiber Bragg gratings (FBG) are the most popular optical pressure measurement methods. The FBG sensor is a specific type of distributed Bragg reflector that is created within a short section of optical fiber. Its function is to selectively reflect certain wavelengths of light while allowing all other wavelengths to pass through. When subjected to strain or temperature variations, the reflected wavelengths of an FBG shift accordingly. The magnitude of this wavelength shift is directly proportional to the applied load. Several scientific papers, including Xiong L. et al. [14] and Guo Yu [16], have documented the development of six-axis force sensors utilizing a fiber Bragg lattice. This design offers several advantages over strain-resistant sensors, such as immunity to electromagnetic interference, a compact profile, and lightweight construction. However, important to note that FBG-based sensors necessitate significant investments in optical signal demodulation equipment [14], as well as surface treatment processes.

3.5.3 Photointerrupter cell with barrier

The optocoupler pressure sensor comprises three main components: a light emitter, two light receivers, and an interrupter positioned between emitter and one of the receivers [15]. When a load is applied to the sensor, the interrupter plate shifts, thereby altering the rate of light intensity on the measuring diode [3]. The signal from the second receiver is a reference and enables the cancellation of the optocoupler characteristics change, that effects whole system equally, caused by temperature, dirt and etc.

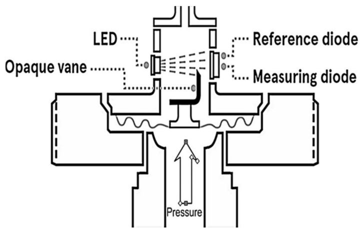

Figure 3.2: Example of an optical pressure sensor

In the mathematical model of this type of cell, the barrier can be considered as a spring, making the applied force proportional to the deformation of the barrier.

This type of sensor has negligible hysteresis and repeatability error, since the vane movement amplitude to close the measuring diode is very small [10]. Additionally, it offers a compact geometry and is cost-effective.

Compared to ERSG sensors, the photointerrupter measurement cell is less susceptible to electrical interference [15].

The properties associated with hysteresis and the sensor's nominal range are primarily influenced by the type of barrier utilized [15].

Other advantages of this type of pressure sensor that are particularly important in some industrial applications are its long transmission distance and the low chemical reactivity of the material, which is ideal for operating in environments with a risk of explosion, in addition to being intrinsically safe [25]. Regarding response time, typical values of this measuring principle can reach values about $100\,\mu$s. [10]

In terms of force, the sensor has an average resolution of 0.1 N over a 200 N measurement range [17].

3.6 Conclusion

In this literature review, we have explored the research conducted by Hosseinabadi and Salcudean [2] and the model proposed by [15] for a mechanically decoupled six DOF force sensor with low cross-coupling error and high resolution to scale ratio of 0.0001%. Additionally, we have examined the 3-DOF force sensor structure proposed in [5], which features four independent beams with an average interference error of less than 3%.

Building upon these previous studies, the current research aims to develop a mechanically decoupled modal structure for a six DOF force sensor, utilizing the measurement cell invented by [15]. The focus of this study will be on calculating the cross-coupling interference, resolution to scale ratio, and hysteresis of the sensor.

Chapter 4

Optical modeling

The main components of the measurement cell are phototransistor (PT), source of light (emitter) and photobarrier (PB). The purpose of the chapter is to find the function $F = f(I_{pt})$, which describes the relation between current on the phototransistor I_{pt} and force F, applied to the barrier.

The current on PT depends on the Illuminance at the phototransistor area. For the project I use a PT module (EE-SX1321, OMRON), it consists of a set of receiver' and emitter' cells [15, Fig. 4]. Therefore, I will calculate the radiant flux for each cell separately.

Optical model of my measurement cell wil be based on the one described in [15].

In the chapter, PB will be simplified to the spring element with aperture. When a force is applied to the PB, the aperture will be shifted relative to the main optical axis of the light source.

Limitations of the mathematical model:

- LED is Lambert's source of light.
- PT acceptable wavelength is the same as of emitted light.

- Light is a stream of particles.
- PB will be simplified to the spring element with aperture. When a force is applied to the PB, the aperture will be shifted relative to the main optical axis of the light source.

Lets start with emitter - in the project the emitter device is light-emitting diode (LED). The device is a semiconductor which transforms electrical power into light [18].

4.1 Simplified model

The force measurement cell can be simplified to model of an spring with barrier and optocoupler.

Radiant intensity on a unit area of the phototransistor:

$$R^2 = (s_1 - x)^2 + (s_2 - y)^2 + l_0^2$$
$$h = \mid y - s_2 \mid$$
$$\beta = \arcsin(\frac{h}{\sqrt{R}})$$
$$I = I_0 * \frac{l_0 \cos \beta}{2 \pi R}$$

R - radius vector from i-th light source to the j-th receiver cell,

β - angle between norm vector of emitter area and the vector R,

s_1, s_2 - coordinates of the LED,

x, y - coordinates of the PT,

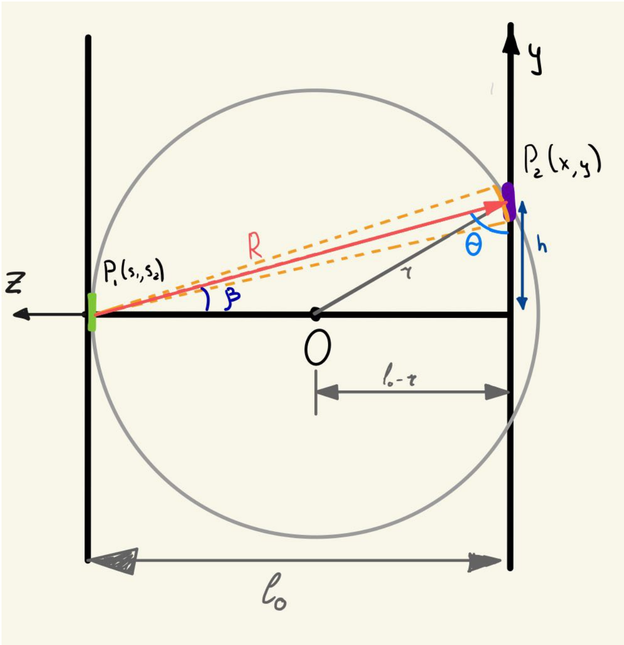

Figure 4.1: The geometrical relationships between LED (green) and PT(purple)

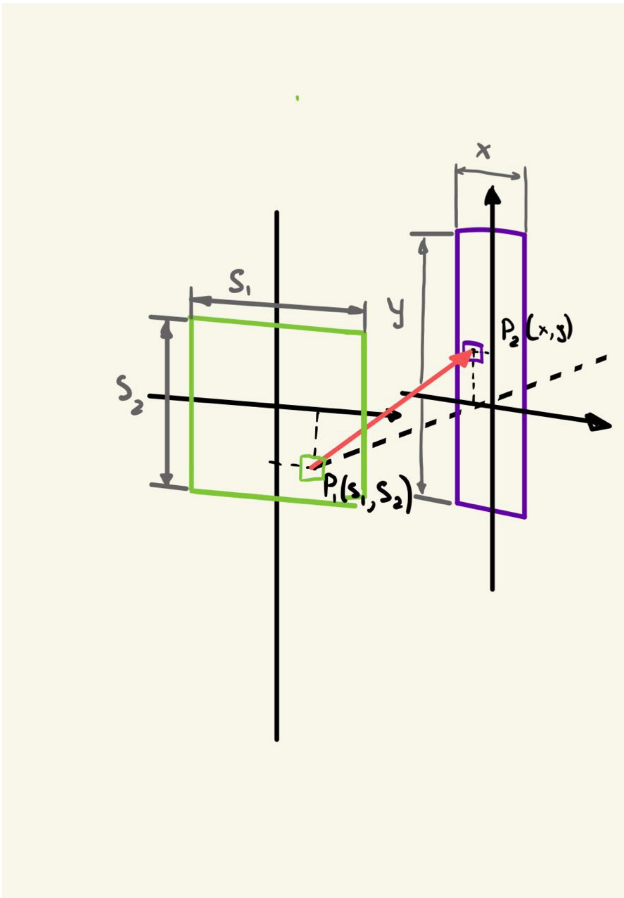

Figure 4.2: LED (green) and photoreceiver (purple) arrangement

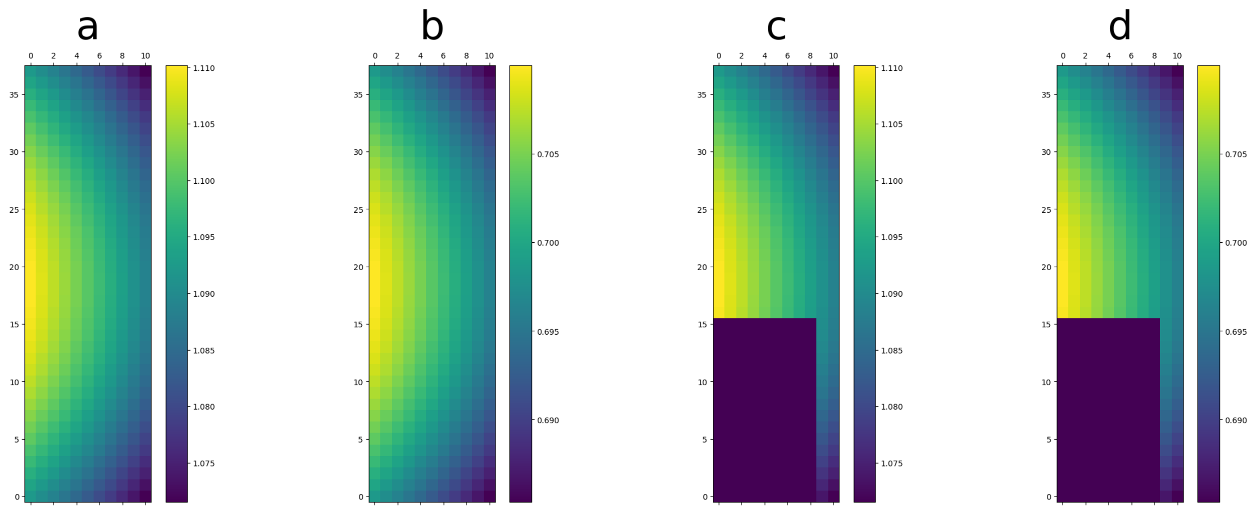

Figure 4.3: Photoreceiver intensity from the formulas: a. The intensity of the

How to calculate the light intensity on the receiver area (flux)?

The model should include area of the emitter and receiver since we measure the current change on the PT

Illuminance estimates the flux received by some area.

Chapter 5

Implementation

This chapter describes the theoretical aspects of six-axial optical force sensor development, the data filtration, communication protocols and the calibration process?

Chapter 6

Results and Discussion

6.1 Results

Bibliography cited

[1] B. B. S. J. O. Templeman and T. Sun, “Multi-axis force sensors: A state-of-the-art review,” *Sensors and Actuators A: Physical*, vol. 304, p. 111 772, 2020, ISSN: 0924-4247. DOI: https : / / doi . org / 10 . 1016 / j . sna . 2019 . 111772. [Online]. Available: https://www.sciencedirect.com/science/article/pii/S0924424719308842.

[2] A. H. H. Hosseinabadi and S. E. Salcudean, “Ultralow noise, high bandwidth, low latency, no overload 6-axis optical force sensor,” *IEEE/ASME Transactions on Mechatronics*, vol. 26, no. 5, pp. 2581–2592, 2021. DOI: 10.1109/TMECH.2020.3043346.

[3] S. Hirose and K. Yoneda, “Development of optical 6-axial force sensor and its signal calibration considering non-linear interference,” *IEEE International Conference on Robotics and Automation*, vol. 1, 1990.

[4] W. Bo and P. Cai, “Decoupling analysis of a sliding structure six-axis force/-torque sensor,” *Measurement Science Review*, vol. 13, no. 4, pp. 187–193, 2013. DOI: https://doi.org/10.2478/msr-2013-0028.

[5] U. Mayetin and S. Kucuk, “A low cost 3-dof force sensing unit design for wrist rehabilitation robots,” *Mechatronics*, vol. 78, p. 102 623, 2021, ISSN: 0957-4158. DOI: https : / / doi . org / 10 . 1016 / j . mechatronics .

2021.102623. [Online]. Available: https://www.sciencedirect.com/science/article/pii/S0957415821001045.

[6] L. P. Chao and K. T. Chen, "Shape optimal design and force sensitivity evaluation of six-axis force sensors," *Sensors and Actuators A: Physical*, vol. 63, no. 2, pp. 105–112, 1997, ISSN: 0924-4247. DOI: https://doi.org/10.1016/S0924-4247(97)01534-3. [Online]. Available: https://www.sciencedirect.com/science/article/pii/S0924424797015343.

[7] H. Cao, Y. Yu, and Y. Ge, "A research of multi-axis force sensor static decoupling method based on neural network," Aug. 2009. DOI: 10.1109/ICAL.2009.5262800.

[8] S. L. M. K. Kang and J. H. Kim, "Shape optimization of a mechanically decoupled six-axis force/torque sensor," *Sensors and Actuators A: Physical*, vol. 209, pp. 41–51, 2014. DOI: https://doi.org/10.1016/j.sna.2014.01.001.

[9] S. M. Nacy, M. A. Tawfik, and I. A. Baqer, "Static and dynamic calibration for flexiforce sensor using a special purpose apparatus," *Innovative Systems Design and Engineering*, vol. 4, pp. 30–40, 2013. [Online]. Available: https://api.semanticscholar.org/CorpusID:118367418.

[10] J. D. Pereira, "Pressure sensors: Working principles of static and dynamic calibration," *Sensors*, vol. 24, no. 2, 2024, ISSN: 1424-8220. DOI: 10.3390/s24020629. [Online]. Available: https://www.mdpi.com/1424-8220/24/2/629.

[11] H. Oh, U. Kim, G. Kang, J. Seo, and H. Choi, "Multi-axial force/torque sensor calibration method based on deep-learning," *IEEE Sensors Journal*, vol. PP, pp. 1–1, May 2018. DOI: 10.1109/JSEN.2018.2834727.

[12] J. Ma and A. Song, "Fast estimation of strains for cross-beams six-axis force/torque sensors by mechanical modeling," *Sensors*, vol. 13, May 2013.

[13] S. Boyn, *Piezoresistive pressure measurement technology, [online]*, `https://www.catsensors.com/media/Archivos_pdf/Fachbeitrag_Piezo_e.pdf`, (accessed Nov. 2, 2023).

[14] G. J. L. Xiong and et. al., "Three-dimensional fiber sensor of the bragg grating friction force for the robot.," *Journal of Information Systems & Operations Management*, vol. 4, no. 2, pp. 99–107, 2010.

[15] Y. C. S. Chong and J. Desai, "Miniature force sensor based on double photo damage with high linearity and interference compensation," pp. 736–747, 2016.

[16] J. K. Y. Guo and et. al., "Three-axis force sensor at the fingertip based on fiber bragg grating," *Sensors and Actuators A: Physical*, vol. 249, pp. 141–148, 2016, ISSN: 0924-4247. DOI: `https://doi.org/10.1016/j.sna.2016.08.020`. [Online]. Available: `https://www.sciencedirect.com/science/article/pii/S0924424716303958`.

[17] S. H. Jeong, H. J. Lee, K.-R. Kim, and K.-S. Kim, "Design of a miniature force sensor based on photointerrupter for robotic hand," *Sensors and Actuators A: Physical*, vol. 269, pp. 444–453, 2018, ISSN: 0924-4247. DOI: `https://doi.org/10.1016/j.sna.2017.11.052`. [Online]. Available: `https://www.sciencedirect.com/science/article/pii/S0924424717309317`.

[18] A. Rammohan, C. Ramesh Kumar, and M. M. Rashidi, "High-power led luminous flux estimation using a mathematical model incorporating the ef-

fects of heatsink and fins," B. Rushi Kumar, R. Sivaraj, B. S. R. V. Prasad, M. Nalliah, and A. S. Reddy, Eds., pp. 429–438, 2019.